

phase mechanisms. The subcooled flow boiling heat transfer has a wide application in refrigeration, micro electro mechanical systems, and nuclear fusion and heat exchanger systems. It can also improve the thermal performance of components in industrial processes.

By using boiling heat transfer method, there will be heat exchanger devices with reduced size like minichannels or microchannel. Kandlikar (2012) has carried out a comprehensive review about the minichannels and microchannels. His review showed that there is no distinct difference between the single phase heat transfer in the microchannel and that in the macroscale channel and he found that the divergences in the literature mainly existed in the two phase boiling which shows the necessity of investigations about the flow boiling inside mini and micro scale channels. Cikim *et al.* (2014) also studied the flow boiling in microtubes with cross linked surface coatings at mass fluxes of 5000 and 20000 kg/m²s. They showed that the coatings enhance boiling heat transfer considerably since more active nucleation sites were made by the porous structure.

In the other hand, one of the methods of heat transfer enhancement inside the channels is to have swirl flow instead of axial flow. In the literature, some researchers have investigated the hydrothermal behavior of swirling boiling flow inside tubes. Among the heat transfer enhancement methods by making swirl flow, the insertion of twisted tape in circular tubes has received much attention. Yagov *et al.* (2005, 2010) investigated the thermal-hydraulic characteristics of subcooled boiling with twisted tape inserts and proposed heat transfer correlations under the condition of uniform heating. Salim *et al.* (2005) investigated experimentally the axial and swirl flow heat transfer in the post critical heat flux region in horizontal tubes. They modified a correlation which better account for the high heat transfer rates at the high mass fluxes. Hata and Masuzaki (2011a, b) studied the subcooled water heat transfer in swirl flow boiling. They found that the heat transfer in twisted tape tubes can be considered the same as that in plain tubes by the introduction of the swirl velocity. Akhavan-Behabadi *et al.* (2009) studied the effect of twisted-tape inserts on heat transfer enhancement during swirl flow boiling of R-134a in horizontal tube. Their results show that the heat transfer coefficient is increased by as much as 57% by insertion of twisted-tapes inside the tube.

The main aim of this study is experimental study of the swirl subcooled flow boiling of deionized water inside mini annular gaps with spring inserts. First, boiling curves and subcooled boiling heat transfer coefficient are presented for the axial flow inside plain mini annular gaps. Second, the variations of single phase heat transfer coefficient and pressure drop by inserting a spring inside a mini annular gap are presented. Then, the boiling curves and subcooled boiling heat transfer coefficients are presented for the swirling flow inside a mini annular gap including spring inserts.

2. EXPERIMENTAL SETUP

2.1. Test Rig

An experimental setup was used to make subcooled flow boiling inside vertical annular gaps for the working fluid of deionized water under the low pressure. The schematic diagrams of the experimental setup at Royal Institute of Technology (KTH) is shown in Fig. 1. The test rig included a gear pump (MCP-Z, Ismatec, Switzerland) with maximum flow rate of 3840 ml/min, and a Coriolis mass flow meter (CMFS015 with 2700 transmitter, Micromotion, Netherlands) with accuracy of 0.1% for the mass flow rate between 167 and 5500 g/min. A cooling jacket has been used in order to cool down the working fluid and adjust the temperature at the inlet of the test section including a 1.7m double tube heat exchanger connected to a thermostat bath (Ecoline Staredition Re204, Lauda, Germany) and a plate heat exchanger (B5H-30, SWEP, Sweden) connected to tap water. Data acquisition units (Agilent 34970A, US) were used to collect and send the data (temperature, pressure difference, mass flow rates and densities) to the computer when the system had reached steady state condition. The Data were recorded every 5s for 200s at steady state condition. A DC power supplier (PSI 9080-100, Elektro-Automatik GmbH, Germany) with maximum power of 3000 Watt was used for applying constant heat flux on the vertical steel tube.

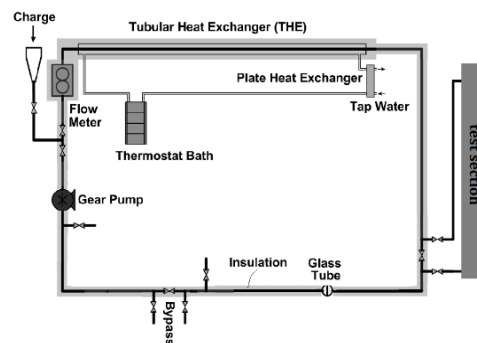
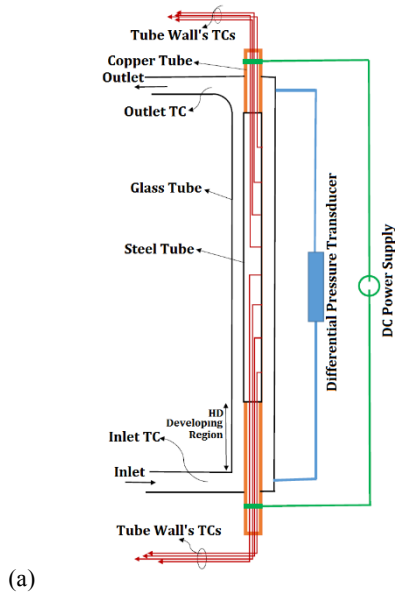


Fig. 1. Schematic of Experimental setup for the subcooled flow boiling test.

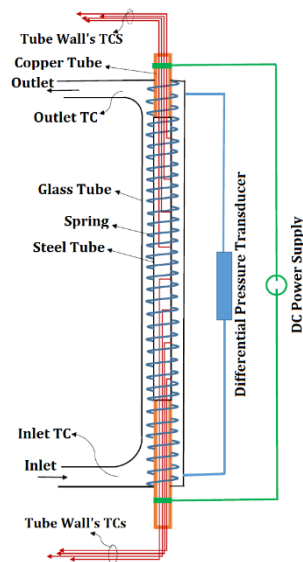
The experiments were carried out by the following procedures. The loop is filled with the deionized water. The deionized water is fully degassed by long-term boiling. The hot water which comes out from the test section is entered and cooled in the heat exchanger. Then, the deionized water is heated/cooled to reach to the required water temperature or subcooling at the inlet of the test section. After setting the mass velocity and inlet subcooling at the required values, the electrical heating system is activated. In all of the experiments, the heat flux was changed in small incremental steps while all of the parameters were kept constant. The system was also allowed to be stabilized before recording of a new data point.

2.2. Test Section

The test section (as seen in Fig. 2-a) consists of a vertical annuli. The inner tube of the annuli is a stainless steel tube with internal diameter of 3.7mm, external diameter of 4mm and length of 320mm. The outer tube of the annuli is a glass tube allowing observation of the flow boiling process with three different internal diameters of 6.8mm, 8mm and 9mm. Thus, three different annular gaps of 1.4mm, 2mm and 2.5mm between the glass tube and steel tube have been considered in this study.



(a)



(b)

Fig. 2. Schematics of the test sections. (a) annuli (b) annuli with spring insert.

The wall temperature measurement of the heated inner steel tube is very important. The thermocouples were installed inside the inner tube. A measurement module for measuring the wall temperature was designed to be inserted inside narrow inner tube

diameter of 3.7mm. The module consisted of eight T-type (0.6 × 1.0 mm) thermocouples (Omega, UK) with accuracy of ±0.1°C designed in such a way that press the thermocouples against the inner tube surface. The axial positions of the thermocouples are $z=32.5\text{mm}$, 67.5mm, 102.5mm, 137.5mm, 172.5mm, 207.5mm, 242.5mm, 277.5mm from the bottom end of the steel tube. Sheathed T-type thermocouples (Omega, UK) with accuracy of ±0.1°C were used for measuring the fluid inlet and outlet temperatures. The pressure drop over the test section was measured by a differential pressure transducer (GE UNIK 5000, 0-2 bar, UK) with accuracy of ±0.0054 bar. The test section also includes an entrance region, ensuring that the flow was fully developed at the beginning of heating section.

The steel tube is heated directly by AC electric current. Both endings of the steel tube are connected to the copper tubes which have connection to cables of the power supply. Thus forming the electrical power supply chain and the vertical stainless steel tube will be exposed to constant heat flux due to Joule effect.

The swirling flow inside the mini annuli will be created by inserting springs inside the mini annuli with the annular gap size of 2mm and the spring will be located at the middle of the outer wall of the steel tube and inner wall of the glass tube without having any contact with them (as seen in Fig. 2-b). The two different used springs in the experiments have the same wire diameter of 0.6mm, coil outside diameter of 6.6mm but they have different pitches of 6mm and 12mm. The clearance in diameter between the inserted spring and the walls of the annular gap is equal to 0.7mm. The length of the inserted springs cover the developing region, the heated section and also the downstream of the heated section. The ends of the springs are also fixed so that the spring will be unmovable by the flow. The spring inserts also have been made electrically insulated by using an insulating coating spray with the commercial name of DCA which is a flexible, transparent and unique modified silicone conformal coating specifically designed for the protection of electronic circuitry.

2.3. Data Reduction

The local convective heat transfer coefficient, h , is defined as:

$$h(z) = \frac{\dot{q}}{T_{w,st,o}(z) - T_m(z)} \quad (1)$$

where z represents the axial distance from the entrance of the test section, \dot{q} is the heat flux applied to the fluid and $T_{w,st,o}(z)$ is calculated as follows:

$$T_{w,st,o}(z) = T_{w,st,i}(z) + \frac{S}{16k_{w,st}} \left[D_{o,st}^2 \ln \left(\frac{D_{i,st}}{D_{o,st}} \right) - (D_{o,st}^2 - D_{i,st}^2) \right] \quad (2)$$

In this equation, S is the amount of the heat per unit volume generated inside the steel tube ($S = 4q/$

$$(\pi L(D_{o,st}^2 - D_{i,st}^2)).$$

The fluid bulk temperature (T_m) is also computed as follows:

$$T_m(z) = T_{in} + \frac{\dot{q}\pi d_{o,st} z}{\dot{m}C_p} \quad (3)$$

where T_{in} is the fluid temperature at the inlet (=34°C).

The applied heat flux to the fluid can be calculated as follows:

$$\dot{q} = \frac{q}{\pi d_{o,st} L} = \frac{VI}{\pi d_{o,st} L} \quad (4)$$

where I and V are current and voltage respectively. Also, heat flux of the fluid can be computed from the following equation:

$$\dot{q} = \frac{\dot{m}C_p}{\pi d_{o,st} L} (T_{out} - T_{in}) \quad (5)$$

Thus, the relative heat loss can be calculated from the following equation:

$$q_{loss}(\%) = \frac{VI - \dot{m}C_p(T_{out} - T_{in})}{VI} \times 100 \quad (6)$$

The average heat transfer coefficients are obtained as the area weighted averages of the local heat transfer coefficients.

2.4. Uncertainty Analysis

An uncertainty analysis is done on the experimental results. The uncertainty of a parameter which is a function of several variables depends on the uncertainties of those variables. The overall uncertainty of the measurement result y obtained from:

$$u_y^2 = \sum_{i=1}^N \left(\frac{\partial f}{\partial x_i} \right)^2 u^2(x_i) \quad (7)$$

According to the above mentioned definition, the relative uncertainties of heat flux and heat transfer coefficient are calculated as:

$$\frac{\delta \dot{q}}{\dot{q}} = \left[\left(\frac{\delta V}{V} \right)^2 + \left(\frac{\delta I}{I} \right)^2 + \left(\frac{\delta(d_o)}{d_o} \right)^2 + \left(\frac{\delta L}{L} \right)^2 \right]^{1/2} \quad (8)$$

$$\frac{\delta h}{h} = \left[\left(\frac{\delta \dot{q}}{\dot{q}} \right)^2 + \left(\frac{\delta T_w}{T_w - T_b} \right)^2 + \left(\frac{\delta T_b}{T_w - T_b} \right)^2 \right]^{1/2} \quad (9)$$

The maximum values for the uncertainty in various experimental parameters are summarized in table 1.

3. RESULTS AND DISCUSSIONS

3.1. Validation

In order to verify the accuracy of the studied experimental system, the experimental results both for the single phase heat transfer and subcooled boiling heat transfer have been compared with correlations in the literature. The obtained experimental results of local Nusselt number for the

single phase laminar mixed convective heat transfer of water flow inside a vertical mini annuli with annular gap size of 2mm and inlet flow temperature of 34°C have been compared with the correlation of the El-Genk *et al.* (2007). As seen in Fig. 3, most of experimental data agree with the predicted value within +/- 10%. The correlation of the El-Genk *et al.* (2007) for the mixed laminar thermally developing upward flow inside a vertical annulus is as follow:

$$Nu_L = (Nu_{F,L}^3 + Nu_{N,L}^3)^{1/3} \quad (10)$$

$$Nu_{F,L} = (Nu_{\infty}^3 + Nu^3)^{1/3} \quad (11)$$

$$Nu = Nu_{\infty} + f(\varepsilon) \left(\frac{0.19 Gz^{0.8}}{1 + 0.117 Gz^{0.4667}} \right) \quad (12)$$

$$Nu_{\infty} = 4.36 + 1.2\varepsilon^{0.8} \quad (13)$$

$$f(\varepsilon) = 1 + 0.14 \varepsilon^{\frac{1}{2}} \quad (14)$$

$$Nu_{N,L} = A \left(\frac{Ra_q}{X} \right)^{0.2} \quad (15)$$

Table 1 Uncertainty values of the important parameters

Parameter	Uncertainty
Steel tube diameter	± 0.01mm
Steel tube length	± 1mm
Glass tube diameter	± 0.05mm
mass flow rate	± 0.1%
temperature	± 0.1 °C
voltage	0.1%
amperage	0.1%
pressure drop	± 0.0054 bar
heat flux	5%
local heat transfer coefficient	7%

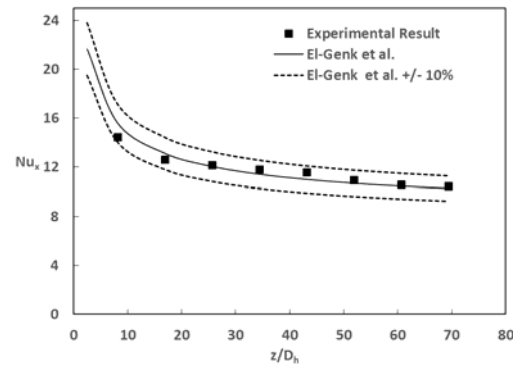


Fig. 3. Comparison of the single phase local Nusselt number with El-Genk's correlation for upward flow inside vertical annuli at inlet temperature of 34°C and Re=625.

The local Nusselt number based on the correlation of EL Genk *et al.* was calculated using thermophysical properties at the average fluid temperature between inlet and outlet.

The obtained experimental results for the subcooled flow boiling inside the vertical annuli with different annular gap sizes at various mass fluxes have also been assessed against the Shah's (2017) correlation

for heat transfer during subcooled boiling in the annuli. The heat transfer in subcooled flow boiling is calculated according to Shah's correlation as follow:

$$q = h_L(T_w - T_B) + h_L(\Psi_0 - 1)(T_w - T_{SAT}) \quad (16)$$

The first term on the right hand side is the heat removed by convection and the second term is the heat removed by nucleate boiling. Ψ_0 is the larger of those given by the following two equations:

$$\Psi_0 = 230Bo^{0.5} \quad (17)$$

$$\Psi_0 = 1 + 46Bo^{0.5} \quad (18)$$

According to Shah Correlation, ΔT_{SAT} is also calculated by following formulas:

In low subcooling regime,

$$\Delta T_{SAT} = \frac{q}{(h_L \Psi_0)} \quad (19)$$

In high subcooling regime,

$$\Delta T_{SAT} = \frac{0.67q}{\Psi_0 h_L} + 1.65(\Delta T_{SC})^{-0.44} \quad (20)$$

The single phase heat transfer coefficient (h_L) in Eq. 16 is also calculated by El-Genk correlation (Eq. 10) for laminar thermally developing upward flow inside an annulus. As seen in table 2, the measured experimental results for different cases are in good agreement with those of predicted by Shah's correlation and the average deviations of the measured heat transfer coefficients from the predicted heat transfer coefficients by Shah' correlation are less than $\pm 15\%$ for the most of the cases.

Table 2 Comparison of the experimental data with Shah' correlation for the subcooled flow boiling heat transfer

Annuli gap	Pr	G	Re	\dot{q}	Average deviation (%)
1.4mm	3.14	150	861	169	-5.92
1.4mm	3.19	90	920	109	-3.59
1.4mm	3.20	115	666	149	-9.62
2mm	3.00	90	800	189	15.47
2mm	3.23	115	983	204	19.48
2mm	3.00	60	521	118	7.88
2.5mm	3.26	90	900	201	14.32
2.5mm	3.2	44	448	113	0.49
2.5mm	3.25	69	690	152	12.32

3.2. Subcooled Flow Boiling Inside Mini Annular Gaps

A boiling curve plots the applied wall heat flux versus the temperature of the heated wall. Fig. 4 shows boiling curves for the mass fluxes of $G=115 \text{ kg/m}^2\text{s}$, $150 \text{ kg/m}^2\text{s}$, $195 \text{ kg/m}^2\text{s}$ at fixed axial positions of $z=242.5\text{mm}$ and 277.5mm for the annular gap size of 1.4mm .

At the beginning, by increasing the heat flux under subcooled liquid condition, the heat transfer occurs by single phase forced convection. Then, the liquid close to the wall soon become superheated, whereas

the flow at the core of the tube still remains subcooled. Further increase in the heat flux results in increased wall superheat, ΔT_{sat} , and eventually in vapor nuclei activation. As the heat flux is increased beyond onset of nucleate boiling, more nucleation sites are activated and small increases in the wall temperature are recorded. It should be added that during the experiments, the occurrence of onset of nucleate boiling was identified by visual observation and also by data of the measured wall temperatures.

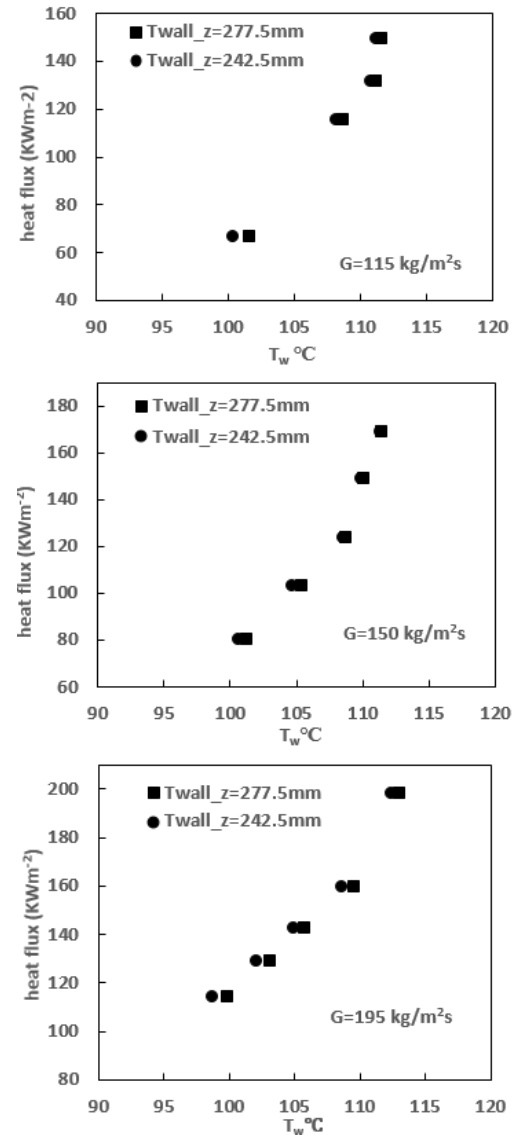


Fig. 4. Boiling curves for $T_{sat} = 100^\circ\text{C}$, $\Delta T_{sub,in} = 66^\circ\text{C}$ inside the annuli with annular gap size of 1.4mm at axial positions of $z=242.5\text{mm}$ and $z=277.5\text{mm}$ for (a) $G=115\text{kg/m}^2\text{s}$, (b) $G=150\text{kg/m}^2\text{s}$, (c) $195\text{kg/m}^2\text{s}$.

Figure 5 compares the boiling curves of three different mass fluxes at the fixed axial position of $z=277.5\text{mm}$ and for the annular gap of 1.4mm . It was seen that the maximum wall superheat is influenced negligibly by mass flux negligibly and the minimum wall superheat required for nucleation is affected by

mass flux. For the lower mass fluxes, lower wall superheat is required to maintain boiling and nucleation over the heated tube and this means that the minimum wall superheat required for nucleation is affected by mass flux. But, the maximum wall superheat reachable during the nucleate flow boiling is almost same for different mass fluxes which means that the maximum wall superheat is influenced negligibly by mass flux.

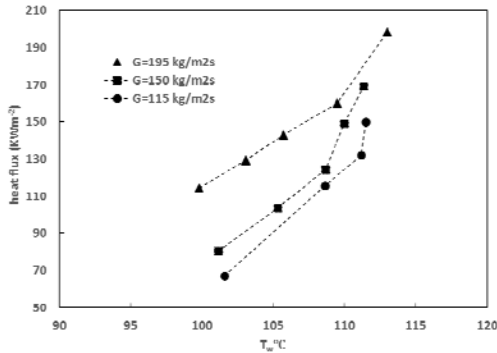


Fig. 5. Boiling curves for $T_{sat} = 100^{\circ}\text{C}$, $\Delta T_{sub,in} = 66^{\circ}\text{C}$ inside the annuli with annular gap size of 1.4mm at axial positions of $z=277.5\text{mm}$.

The effect of the size of the annular gap on the subcooled flow boiling heat transfer coefficients at a fixed axial position of $z=277.5\text{mm}$ for the mass flux of $G=90\text{ kg/m}^2\text{s}$ is shown in Fig. 6. As shown, the subcooled boiling heat transfer coefficient for a given heat flux increases as the size of the annular gap is decreased.

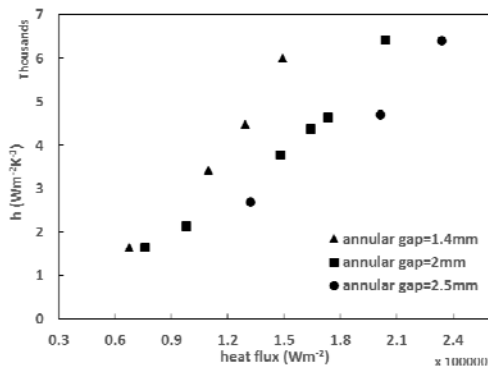


Fig. 6. Effect of the size of the annular gap on the subcooled flow boiling heat transfer coefficients at a fixed axial position of $z=277.5\text{mm}$ and the mass flux of $G=90\text{ kg/m}^2\text{s}$.

Figure 7 shows the variation of the local subcooled flow boiling heat transfer coefficient along the length of the annuli for two different annular gap sizes of 2mm and 2.5mm under applied heat flux of 201000 W/m^2 . As seen, unlike the single phase condition which is accompanied by slight decrease in heat transfer coefficient with increase of axial distance from the inlet, the heat transfer coefficient for the boiling condition within the subcooled region is

increased with increase of axial distance from the inlet. Moreover, as the axial distance from the entrance of the annuli is increased, the increase in local subcooled boiling heat transfer coefficient for the smaller annular gap (2mm) is much higher than that of larger annular gap (2.5mm).

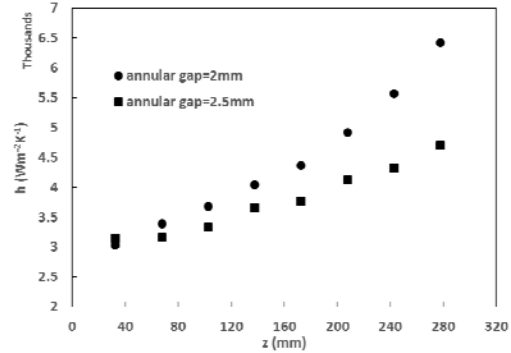


Fig. 7. Variation of the local subcooled boiling heat transfer coefficient along the length of the annuli for $G=90\text{kg/m}^2\text{s}$ and $\dot{q} = 201000\text{ W/m}^2$.

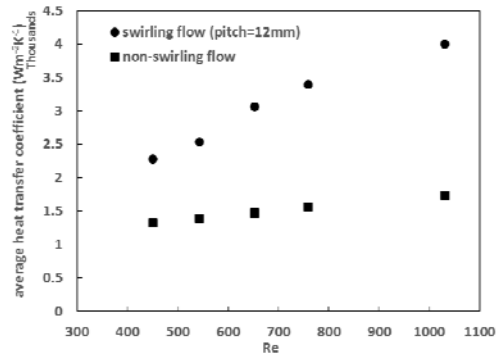


Fig. 8. Variations of the average single phase heat transfer coefficient by insertion of spring with pitch of 12mm inside the mini annuli.

3.3. Effects of Swirl Flow Generated by Spring Inserts on the Single Phase and Subcooled Boiling Heat Transfer

Figure 8 shows the variations of the average single phase heat transfer coefficient by insertion of a spring with pitch of 12mm inside the annuli for different Reynolds numbers. As seen, the average heat transfer coefficient has been increased considerably by having swirl flow inside the annuli. The percent of enhancement in average heat transfer coefficients by having swirl flow inside the mini annuli by using spring insert have been shown in Fig. 9. As predicted, the enhancement has been increased with increase of the Reynolds number. By insertion of spring inside the mini annuli, the centrifugal force is exerted on the moving fluid. Thus, the mixing between the fluid in the core and fluid near the heated wall is increased and the thermal boundary layer is decreased and consequently the heat transfer will be increased. Fig. 10 shows the percent of increase in total pressure drop by inserting spring inside the annuli to make the swirling flow inside the annuli. The single phase thermal performance of the annuli

with spring insert can be defined as the performance ratio of $(\frac{Nu}{Nu_0})/(\frac{dp}{dp_0})^{1/3}$ and this value is 2.078 for the single phase flow with the Reynolds number of $Re=1030$ which shows that the annuli with spring insert perform much better than plain annuli.

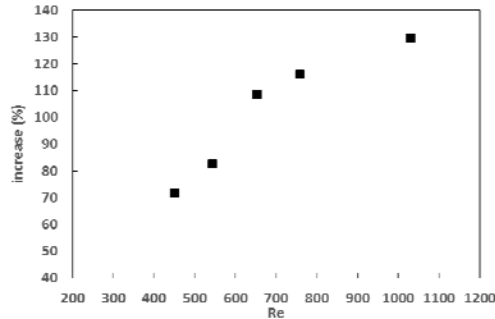


Fig. 9. Average enhancement in single phase heat transfer coefficient by having swirling flow inside the mini annuli using spring insert with pitch of 12mm.

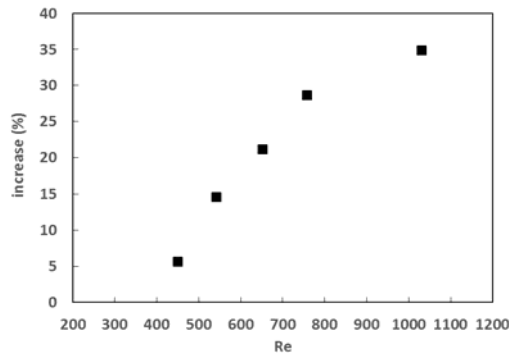


Fig. 10. Increase in total pressure drop by insertion of spring with pitch of 12mm inside the mini annuli.

In the next step, the effects of swirl flow generated by spring inserts inside the annuli on the subcooled boiling heat transfer have been studied. Fig. 11 compares the values of the subcooled boiling heat transfer coefficient at a fixed axial position of $z=277.5\text{mm}$ for the plain annuli and the annuli including springs with different pitches at mass flux of $G=90\text{ kg/m}^2\text{s}$. As seen, the local boiling heat transfer coefficients have been increased by having swirl flow inside the annuli and the enhancement is higher for the spring insert with lower pitch. Moreover, in the single phase and early subcooled boiling, h , is strongly dependent on the swirling intensity of the flow but the enhancement of heat transfer by having swirl flow decreases as the applied heat flux is increased. For higher heat fluxes in subcooled boiling region, the boiling heat transfer coefficient is approximately independent from the swirl effects generated by spring inserts.

The dependence of the subcooled boiling heat transfer coefficient on the mass flux of the swirling flow inside the annuli including spring insert (pitch=12mm) at a fixed axial position of $z=277.5\text{mm}$ has been shown in Fig. 12. As seen, the heat transfer coefficient is clearly a function of the

mass flux for a given value of \dot{q} . In the subcooled boiling heat transfer region, the wall temperature remains almost constant and very small increases occurs in the wall temperature. Thus, as the mass flux is decreased in this region of heat transfer (subcooled boiling heat transfer), the mean temperature of the fluid increases while the wall temperature remains almost constant. Thus, according to the heat transfer coefficient definition, the heat transfer coefficient will be increased.

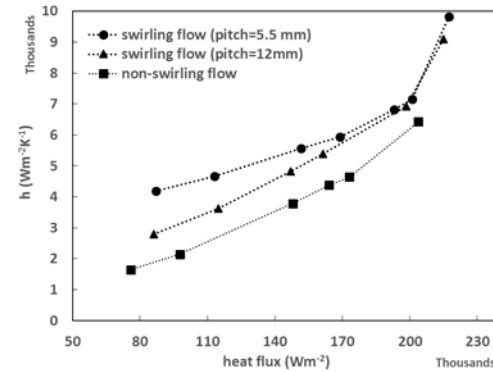


Fig. 11. Effect of swirling flow inside the annuli generated by spring inserts with different pitches on the subcooled flow boiling heat transfer coefficients at a fixed axial position of $z=277.5\text{mm}$ for a mass flux of $G=90\text{ kg/m}^2\text{s}$.

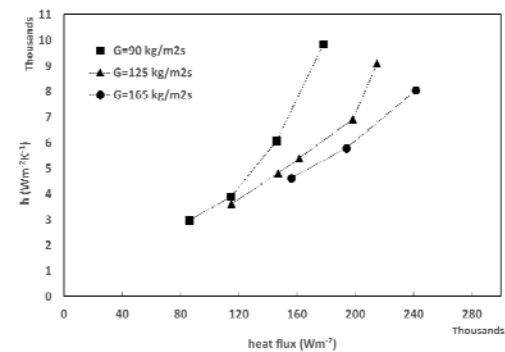


Fig. 12. Effect of mass flux on the subcooled boiling heat transfer coefficient of the swirling flow inside the annuli at a fixed axial position of $z=277.5\text{mm}$.

Figure 13 depicts the effects of the spring inserts on the local subcooled boiling heat transfer coefficient along the length of the annuli for the applied heat flux of 201000 W/m^2 and at mass flux of $G=90\text{ kg/m}^2\text{s}$. As seen, by making swirling flow inside the annuli using spring insert, the local heat transfer coefficients have been increased along the length of the annuli so that the maximum and minimum measured local enhancement in heat transfer coefficient along the length of the annuli by using spring insert with the pitch of 6mm inside the annuli are 33.9% and 9.55% respectively for the mass flux of $G=90\text{ kg/m}^2\text{s}$ and the applied heat flux of 201000 W/m^2 . At the entrance region of the annuli which is a very low void subcooled boiling region, the nucleate boiling contribution is small and the heat transfer coefficient is therefore strongly dependent on the swirling

intensity of the flow. As the distance from the inlet is increased, more nucleation sites are activated, the contribution to heat transfer from the nucleate boiling continues to rise while the single phase convection contribution diminishes. Moreover, the rate of enhancement in local heat transfer coefficient due to spring inserts inside the annuli is decreased as the distance from the inlet of the annuli is increased.

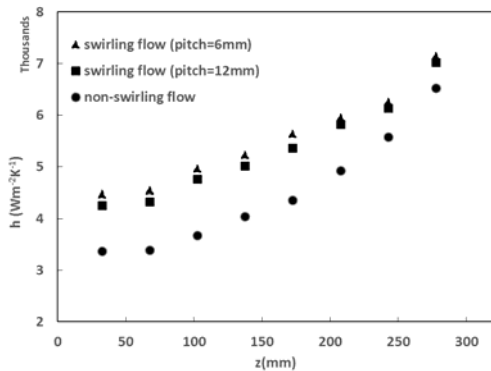


Fig. 13. Effects of swirling flow generated by spring inserts with different pitches on the local subcooled boiling heat transfer coefficient along the length of the annuli for $\dot{q} = 201000 \text{ W/m}^2$ and $G=90\text{kg/m}^2\text{s}$.

4. CONCLUSION

This paper involves experimental investigation of subcooled boiling heat transfer of axial and swirling deionized water flow inside vertical mini annular gaps at atmospheric pressure. The boiling curves and subcooled boiling heat transfer coefficient were presented for flow inside plain mini annuli with different annular gap sizes. The experimental results for the axial flow inside mini annular gaps showed that the minimum wall superheat necessary for nucleation is affected by mass flux while the maximum wall superheat is affected very slightly by mass flux. Moreover, the subcooled boiling heat transfer coefficient for a given heat flux increases as the size of the annular gap is decreased.

The swirling flow inside the mini annuli was made by inserting springs inside the mini annuli with annular gap size of 2mm and the effects of swirl flow due to spring inserts on the single phase and subcooled flow boiling heat transfer were studied and the boiling curves and subcooled boiling heat transfer coefficient were presented for the flow inside a mini annular gap including spring inserts.

The experimental results showed that the single phase and subcooled boiling heat transfer coefficient are increased by using spring inserts and the enhancement is higher for the spring insert with lower pitch. Furthermore, the enhancement of the subcooled boiling heat transfer due to swirl effects decreases as the applied heat flux is increased in the subcooled heat transfer region.

REFERENCES

- Akhavan Behabadi, M. A., R. Kumar and M. Jamali (2009). Investigation on heat transfer and pressure drop during swirl flow boiling of R-134a in horizontal tube. *Int. J. Heat Mass Transfer* 52, 1918-1927.
- Cikim, T., E. Armagan, G. O. Ince and A. Kosar (2014). Flow boiling enhancement in microtubes with crosslinked pHEMA coatings and the effect of coating thickness, *J. Heat Transfer-Trans. ASME* 136, 081504-081504-11.
- El-Genk, M. S. and D. V. Rao (2007). Heat transfer experiments and correlations for low Reynolds number flows of water in vertical annuli, *Heat Transfer Engineering* 10(2), 44-57.
- Hata, K. and S. Masuzaki (2011a). Heat transfer and critical heat flux of subcooled water flow boiling in a SUS304-tube with twisted-tape insert, *J. Therm. Sci. Eng. Appl.* 3, 012001-012001-12
- Hata, K. and S. Masuzaki (2011b). Twisted-tape-induced swirl flow heat transfer and pressure drop in a short circular tube under velocities controlled, *Nucl. Eng. Des.* 241, 4434-4444.
- Kandlikar, S. G. (2012). History, advances, and challenges in liquid flow and flow boiling heat transfer in microchannels: a critical review, *J. Heat Transf* 134 (3), 34001.
- Salim, M. M. and D. M. France (2005). Post-CHF axial and swirl flow heat transfer in small horizontal tubes, *Journal of thermophysics and heat transfer* 19, 163-171.
- Shah, M. M. (2017). New correlation for heat transfer during subcooled boiling in plain channels and annuli, *International Journal of Thermal Sciences* 112, 358-370.
- Yagov, V. V. (2005) Heat transfer and crisis in swirl flow boiling, *Exp. Therm. Fluid Sci* 29, 871-883.